DESY HERA 87-04
February 1987

FIRST RESULTS FROM THE LEBT WITH H^- SOURCE

by

H.S. Chang, G.-G. Winter
Deutsches Elektronen-Synchrotron DESY, Hamburg,

H.Krause, N.Schirm and I.Teßmann
I.Institut für Experimentalphysik, Universität Hamburg.

First results from the LEBT with H^- source.

During 1986 the low energy beam transport (LEBT) and the emittance measurement facility became operational and have been installed in the LINAC tunnel together with the H^- source. In the following we report on:

(1) Beam centering and shielding of the fringe field of the source magnet.

(2) Tuning of LEBT.

(3) Measurement with the emittance facility.

(4) Some consequences on the H^- source.

We first briefly describe the apparatus. It is shown in fig. 1. Details are given in ref. [1]. The LEBT consists of two identical solenoids of 17 cm mechanical length. The distance between both is 17 cm and the first is positioned 15.4 cm behind the exit of the source deflection magnet. Two slit-multiwire emittance heads for x and y can be mounted in three positions:

(a) At the position of the first solenoid after this has been removed.

(b) Between the two solenoids (first beam focus). This position can be permanently used during normal operation.

(c) Behind the LEBT. Here the LEBT has to be disconnected from the RFQ and moved backward on its movable support together with the source. Alternatively a Faraday cup can be installed here.

The system is pumped by two turbo pumps, - one (1000 l/sec) on top of the source housing and an other (1500 l/sec) between the two solenoids. Normally the pressures for 10 Hz operation of the magnetron are $P_{source} \simeq 0.9 \times 10^{-5}$ mbar and $P_{LEBT} \simeq 4 \cdot 10^{-6}$ mbar respectively.

1. Beam centering and shielding of the fringe field of the source bending magnet.

The position and direction of beam center (x_0, x'_0, y_0, y'_0, with y perpendicular to the bending plane of the source magnet) has been measured by the emittance facility in position (b). For y we measured $y_0 = -0.4 \pm .1$ mm, $y_0' = 1 \pm 0.5$ mrad. This result indicates that the mechanical alignment of the system is good. For x the center depends on the setting of the bending magnet.

Fig. 2 shows x_0 versus x'_0 for different magnet currents. For a beam with $x'_0 = 0$ we observe a displacement of $x_0 \simeq +11$ mm (curve a, measured between the solenoids); i.e. the beam center is outside of the nominal bending circle. This displacement is caused by the fringe field of the source magnet, which induced a rather strong field ($\sim$ 50 G) inside the first solenoid. In order to shield the fringe field we used a 60x60 cm^2 iron plate, 1 cm thick, with an 5 cm circular opening for the beam pipe. The optimal position of the plate was found to be in front of solenoid 1. Fringe field measurements with and without the shielding plate are shown in fig. 3. The beam displacement measured immediately behind the iron plate is now only -1 mm for $x'_0 = 0$ (curve b in fig. 2). Later measurements have shown, that the displacement of the emittance center in x and y is smaller than 1.4 mm and 11 mrad between the solenoids and smaller than 0.3 mm and 2.5 mrad at the RFQ position. When passing through a solenoid with nominal current settings x and y displacements are interchanged by a rotation of about 90°.

We observed that a magnetic field is induced inside the solenoid by an external magnetic field. The direction of the induced magnetic field is almost the same as the external magnetic field. So it is possible to steer the beam by putting a permanent magnet at a proper position on the solenoid. We have observed that the focused current could be increased from 24 mA to 26 mA by this way.

2. Tuning of the LEBT.

The LEBT was designed to focus the divergent beam of the source with an assumed emittance of $x_{max} = 0.75$ cm, $x'_{max} = 37$ mrad, $\varepsilon_N = .1\ \pi$ cm mrad into the RFQ with an assumed acceptance of $x_{max} = 0.18$ cm, $x'_{max} = 102$ mrad, $\varepsilon_N = .1\ \pi$ cm mrad. In addition symmetry in x and y is assumed [1]. From beam transport calculations we expected, that currents up to 20 mA can be matched, for higher currents space charge neutralization is necessary. The setting of the solenoids depends on the amount of space charge neutralization [1].

We have measured beam profiles and emittances at the exit of the source with a Faraday cup and a pepper pot [2, 4] and later with the emittance apparatus [3]. Fig. 4 shows a typical emittance measurement for a $\sim$ 40 mA beam, measured behind an additional diaphragm of 25 mm diameter (only for this measurement).

The ellipse parameters are:

ε_{xN} = 0.15 π cm mrad, x_{max} = 1.6 cm, x'_{max} = 97 mrad

ε_{yN} = 0.10 π cm mrad, y_{max} = 1.3 cm, y'_{max} = 53 mrad

ε_N is the normalized emittance calculated for 90 % of the observed current. All measurements have shown, that the emittance is asymmetric in x and y and larger than assumed. The asymmetry is caused by the geometry of the magnetron extraction slit. Only the central part of the beam (r = < .75 cm) approximately has the assumed properties. It contains about 30 mA.

At the LEBT exit we first measured with a Faraday cup, which was designed to simulate the RFQ acceptance. This measurement was used for tuning the LEBT. Later the cup was removed to measure with the emittance apparatus at the RFQ's position. The Faraday cup is shown in fig. 5. To simulate the RFQ acceptance the beam has to pass a channel before it enters the cup. The dimensions of the channel are: 16.4 mm in length with an aperture of r = 1.8 mm at both ends and r = 1.45 mm in the middle. These dimension have been checked by beam transport calculations including space charge forces. To judge the symmetry of the beam, the entrance diaphragm is divided into four quadrants. The beam current collected by these quadrants (A, B, C, D), the channel (E) and the cup (F) can be measured separately. For technical reasons in the following we give only results for the sum i_E+i_F, i.e. the central part of the beam without angular restrictions [5]. Later we comment on the fraction i_E/i_{E+F}. We have tuned the LEBT by optimizing the settings of the solenoid currents i_{S1}, i_{S2} and the bending current of the source (i_B) for a maximum beam current on cup E and as equal currents on cups A, B, C, D as possible. The results near optimum conditions are shown in fig. 6 together with the signal from the beam toroid at the source exit. The most striking observation is the different time dependence of the signals collected from the outer part of the beam (A+B+C+D) (curve a) compared to the central part (E+F) (curve b). This behaviour is caused by space charge neutralization: The first part of the beam (∿ 20 μsec) is completely lost, then neutralization becomes slowly effective and a moderate focus of the beam is obtained. Only the last part of the beam finds stable conditions: About 32 mA (i.e. 64 % of the extracted beam) can be focused into cups E and F. The rise time for this signal is about 90 μsec, the width of the flat top is ∿ 15 μsec. The width can be increased by a longer beam pulse. Of course one can focus the earlier part of the beam onto the cups E+F by increasing the current of the solenoids, but stable conditions can be achieved only after ∿ 90 μsec for the last part.

Space charge neutralization depends on the pressure. To demonstrate this we show in fig. 7 the signal i_E+i_F for two different pressures ($p_1 = 2 \cdot 10^{-5}$ mbar, $p_2 = 9 \cdot 10^{-6}$ mbar): For the higher pressure a shorter rise time is observed.

We add two comments to characterize the individual behaviour of cups A through F:

- The current onto the quadrants B+D is more than twice that on A+C for a good setting of the current. This is a consequence of the asymmetry of the source.
- The part of the beam lost in the channel (i_E) is about 15 % of i_F+i_E. In other words: For 85 % of the central beam spot (r < 1.8 mm) the convergence angle is < 102 mrad. This is what one expects from the focusing geometry of solenoid 2.

The dependence of transmitted current i_{E+F} on the settings of the solenoids and the bending current is shown in fig. 8. The values for optimum transmission are: $i_{S1} \simeq 375$ A, $i_{S2} \simeq 395$ A, $i_B \simeq 7.3$ A. Typically, a missmatch of one of the three parameters by ∿ 2 % results in a decrease of intensity by ∿ 10 %.

In conclusion: The current fraction observed with the simulated RFQ acceptance with and without angular limitation is 54.5 % and 64 % respectively for an extracted current of ∿ 60 mA. Due to space charge effects we expect a dependence of the transmission ratio (i_F/i_b) on the extracted current (i_b). We have observed that for a higher extracted current the transmission ratio is lower. More accurate measurements will be made later.

The above results are obtained for equal polarity of the solenoids. For opposite polarity we observe a decrease of the current i_{E+F} by about 30 %. This indicates that the centering of both solenoids is not perfect.

3. Measurements with the emittance facility.

For the emittance measurements, which we will discuss now, the settings of the solenoids and the bending magnet is kept on the optimum condition found with the Faraday cup. In fig. 9 we show the measured y-emittance contours (90 % of the total observed current is inside the contours) at sample times of 30, 70, 90 and 120 μsec relative to arc start time. Also shown is the expected RFQ acceptance.

We observe a strong dependence of the emittance on time, as expected from the Faraday cup measurements. It is evident that the matching of emittance and acceptance improves with increasing sample time. But even for sampling times exceeding 90 µsec an appreciable part of the beam is outside of the expected RFQ acceptance.

Fig. 10 shows x and y contours at a sampling time of 100 µsec. The corresponding parameters are:

$$\varepsilon_{xN} = 0.20\ \pi \text{ cm mrad},\ x_{max} = 0.28 \text{ cm},\ x'_{max} = 132 \text{ mrad}$$

$$\varepsilon_{yN} = 0.14\ \pi \text{ cm mrad},\ y_{max} = 0.29 \text{ cm},\ y'_{max} = 134 \text{ mrad}$$

Again, ε_N is the normalized emittance calculated for 90 % of the transmitted current (note that the diaphragm was not limiting in this measurement).

The total transmitted current itself is about 85 % of the extracted current measured with the beam toroid. To evaluate the percentage of the beam, which matches the RFQ acceptance, the dependence of emittance parameters on the beam fraction has been calculated by the analysis program, as shown in fig. 11. From this we can conclude that about 62.5 % of the observed current for x and y is simultaneously inside the RFQ acceptance ellipse. The ellipse parameters accepted by the RFQ are:

$$\varepsilon_{xN} = 0.09\ \pi \text{ cm mrad},\ x_{max} = 0.18 \text{ cm},\ x'_{max} = 93 \text{ mrad}$$

$$\varepsilon_{yN} = 0.06\ \pi \text{ cm mrad},\ y_{max} = 0.14 \text{ cm},\ x'_{max} = 100 \text{ mrad}$$

The ellipses are shown in fig. 12.

Finally we show in fig. 13 the result of an emittance measurement between the two solenoids. Comparing this with fig. 9 we observe that x and y are interchanged when passing the second solenoid due to the rotation by the solenoid.

In conclusion: At least 62.5 % of the transmitted current, i.e. about 51 % of extracted current, are inside the expected RFQ acceptance. This is in good agreement with the fraction of 54 % found with the Faraday cup.

4. Some consequences on the source.

(a) The most important change of parameters due to the above observations is an increase of the arc pulse width from 90 µsec to 140 µsec. This allows us to produce a stable beam with a ∿ 50 µsec flat top at the exit of the LEBT.

Although the pulse forming network of the arc pulser was designed for a maximum pulse length of 90 µsec, we get acceptable arc pulses of 140 µsec length for currents up to about 80 mA.

(b) The increased arc pulse width produces more heat inside the magnetron. We therefore reduced the repetition rate (H_2 injection and arc) from 15 Hz to 8 Hz.

(c) The beam is extracted once per second, independent of the repetition rate of the magnetron.

(d) To shorten the long beam pulse rise time (τ_r) caused by space charge neutralization, we have increased the delay time τ_d between gas pulse and arc pulse. The delay allows the beam to pass the LEBT when the pressure burst of the H_2 injection has its maximum inside the LEBT. Fig. 14 shows the measured dependence of the beam pulse rise time on the delay time. For optimum magnetron operation a delay of 650 µsec was found. Considering the effect of space charge neutralization τ_d = 1000 µsec is used now.

(e) Occasionally, we observed a very noisy beam from the source. These oscillations were much enlarged during transport through the LEBT, and also by increasing the pressure of the LEBT. We do not yet completely understand the origin of these oscillations, but they seem to be related to be arc current. This is shown in fig. 15. For currents larger than 60 A the beam modulation $M = \Delta i/i$ is smaller than ± 5 %.

(f) The refrigerator for the coldbox is now installed. The temperature of the box is -40° C. It is monitored and if a threshold of -30° C is exceeded, the valve between the two solenoids will be closed to prevent cesium from entering the RFQ.

References

[1] U. Timm et al., Project study for the 50 MeV HERA Linac, DESY-HERA 84-12

[2] R. Wagner, G.-G. Winter, Status of the H^- source, PLIN-Note 86-05

[3] I. Teßmann, Untersuchungen zur Emittanz der HERA-Ionenquelle, Diplomarbeit, Hamburg 1986, DESY-HERA 86-16

[4] R. Wagner, Bau und Test einer Ionenquelle für HERA, Diplomarbeit, Hamburg 1986, DESY-HERA 87-03

[5] We started the measurements with a channel of length 28 mm. This resulted in an angular acceptance which was to small. Later we continued with the proper channel lengh (16.4 mm) but most of the tuning measurements have not been repeated systematically due to lack of time. The sum i_E+i_F is independent of the channel length.

Figure caption

Fig. 1 Layout of the LEBT with the H^- source and emittance head.

Fig. 2 Direction (x'_0) versus position (x_0) of the beam center.
curve (a): without shielding, measured between the solenoids.
curce (b): with a 1 cm iron plate for shielding, measured behind the shielding plate.

Fig. 3 Fringe field at the source exit with (a) and without (b) shielding.

Fig. 4 A typical beam emittance for x and y at the position of the first solenoid.

Fig. 5 Layout of the Faraday cup used for tuning the LEBT.

Fig. 6 Time dependence of the currents observed with the Faraday cup at the RFQ's position.
curve (a): current collected from the outer part of the beam ($i_A+i_B+i_C+i_D$).
curve (b): central part of the beam (i_E+i_F).
curve (c): total transported current (sum of (a) and (b)).

Fig. 7 Dependence of the beam risetime on pressure demonstrated with an oscilloscope picture of the current observed with the Faraday cup (E+F). The pressures are $2 \cdot 10^{-5}$ mbar (a) and $9 \cdot 10^{-6}$ mbar (b).

Fig. 8 Dependence of the currents observed with the Faraday cups E+F on the solenoid current (a) and the bending current (b).

Fig. 9 The y emittance measured at different sample times at the RFQ's position.

Fig. 10 The x and y emittance at a sample time of 100 µsec at the RFQ's position.

Fig. 11 Dependence of the emittance parameters on the fraction (F) of current inside the contours.

Fig. 12 x and y emittance contours matched to the RFQ acceptance. The contours contain 62.5 % of observed current.

Fig. 13 x and y emittance between the solenoids at a sample time of 100 µsec.

Fig. 14 Dependence of the beam pulse risetime observed with Faraday cup on the delay between gas injection and arc start.

Fig. 15 Modulation of the beam current (M) versus arc current.

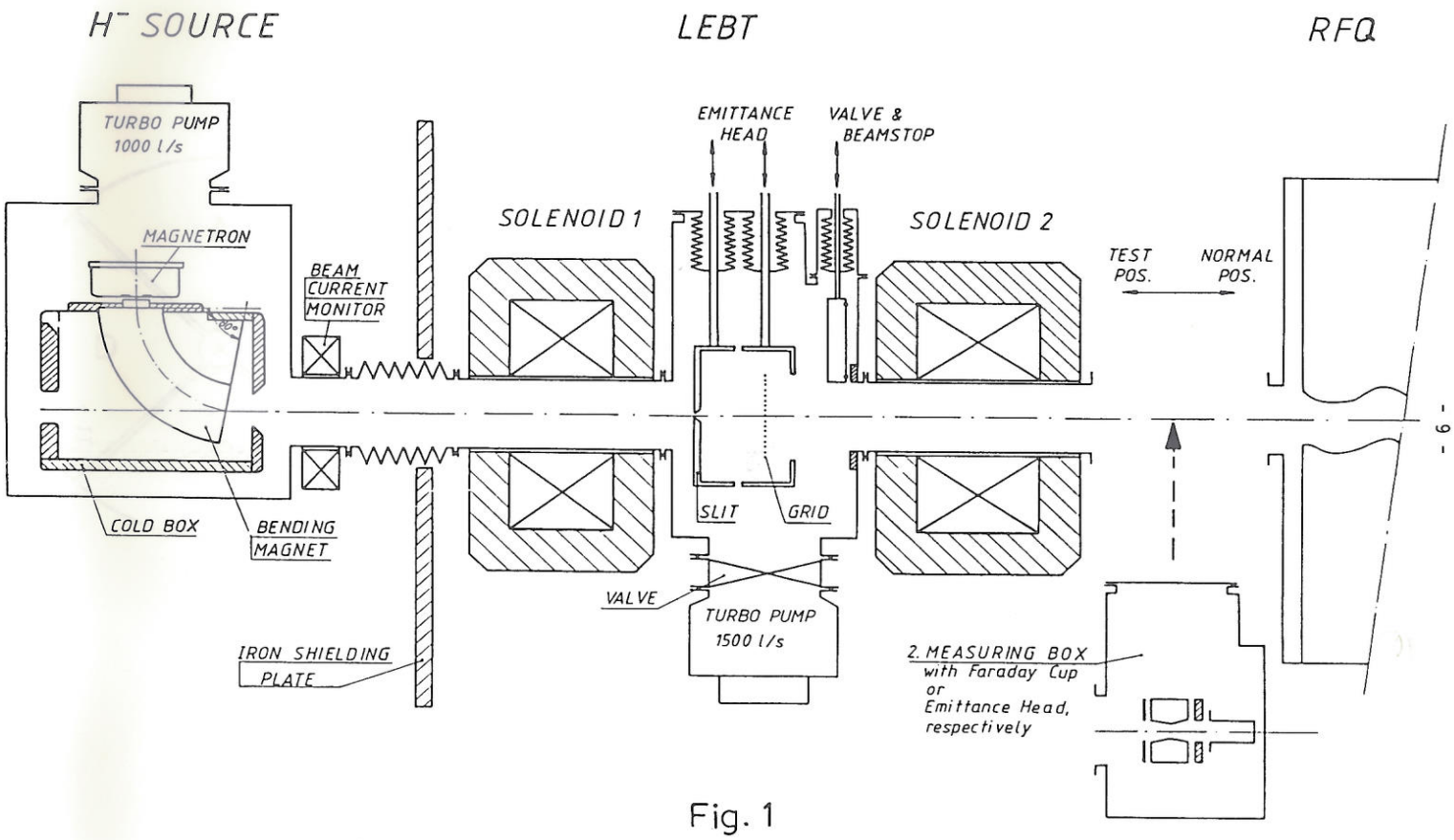
H⁻ SOURCE
LEBT
RFQ
TURBO PUMP
1000 l/s
MAGNETRON
BEAM
CURRENT
MONITOR
SOLENOID 1
EMITTANCE
HEAD
VALVE &
BEAMSTOP
SOLENOID 2
TEST
POS.
NORMAL
POS.
COLD BOX
BENDING
MAGNET
SLIT
GRID
VALVE
TURBO PUMP
1500 l/s
IRON SHIELDING
PLATE
2. MEASURING BOX
with Faraday Cup
or
Emittance Head,
respectively

Fig. 1

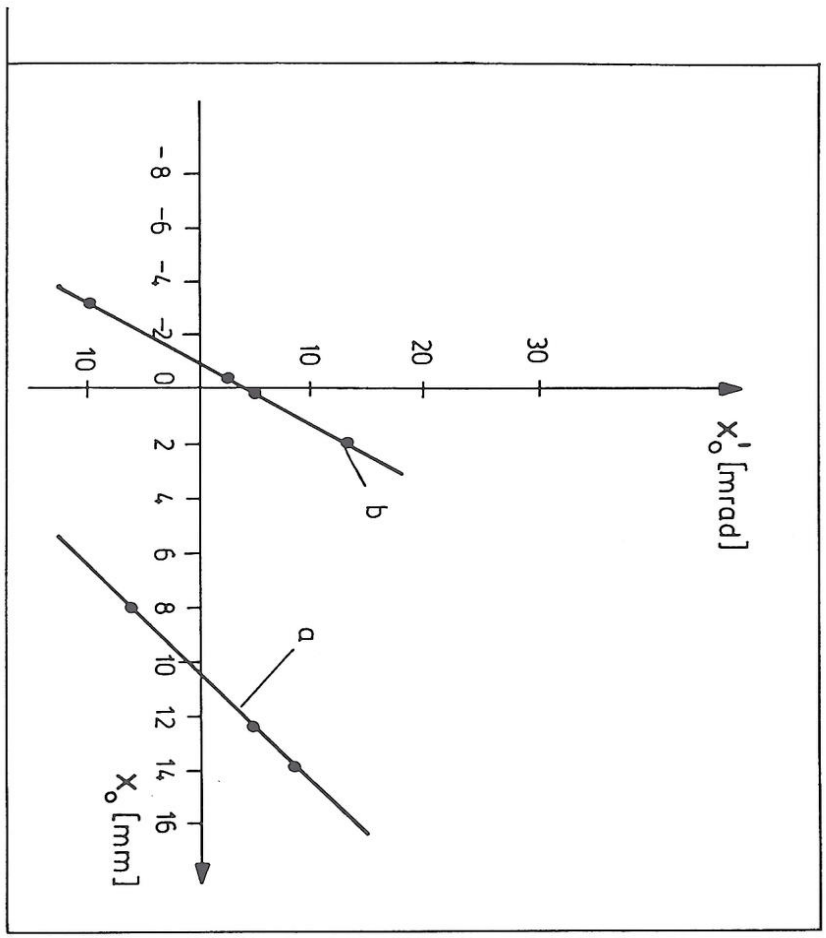
-8
-6
-4
-2
0
2
4
6
8
10
12
14
16
10
10
20
30
x_o [mm]
x_o' [mrad]
a
b

Fig. 2

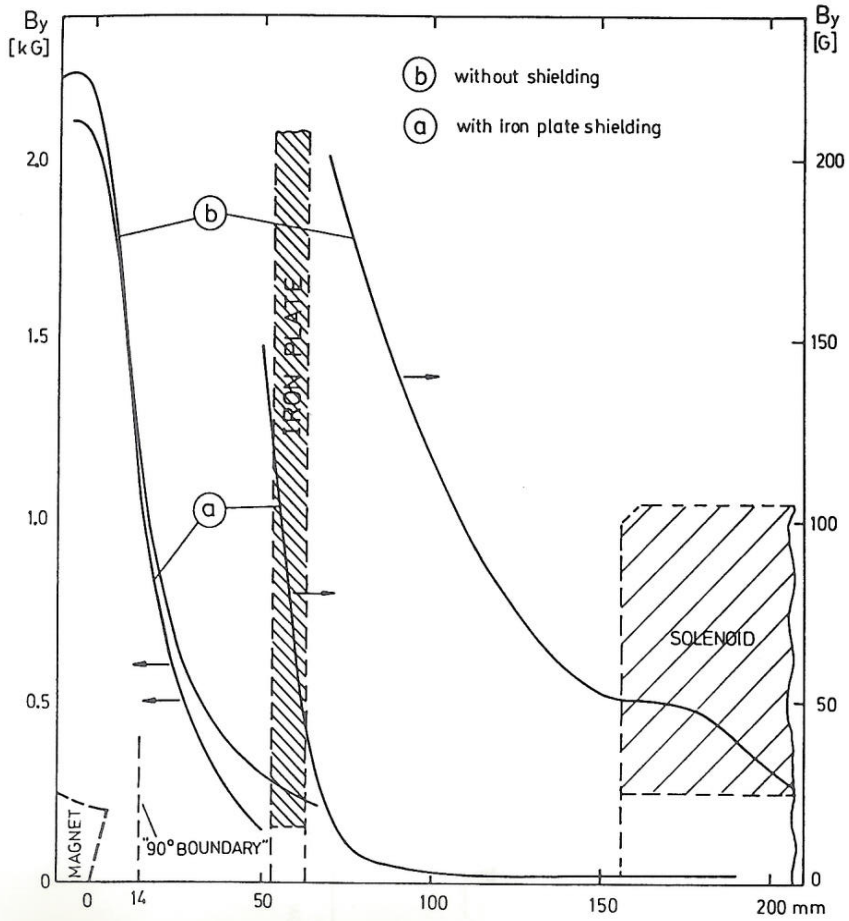
By
[kG]
By
[G]
b without shielding
a with Iron plate shielding
IRON PLATE
SOLENOID
MAGNET
"90° BOUNDARY"
2.0
1.5
1.0
0.5
0
200
150
100
50
0
0
14
50
100
150
200 mm

Fig. 3

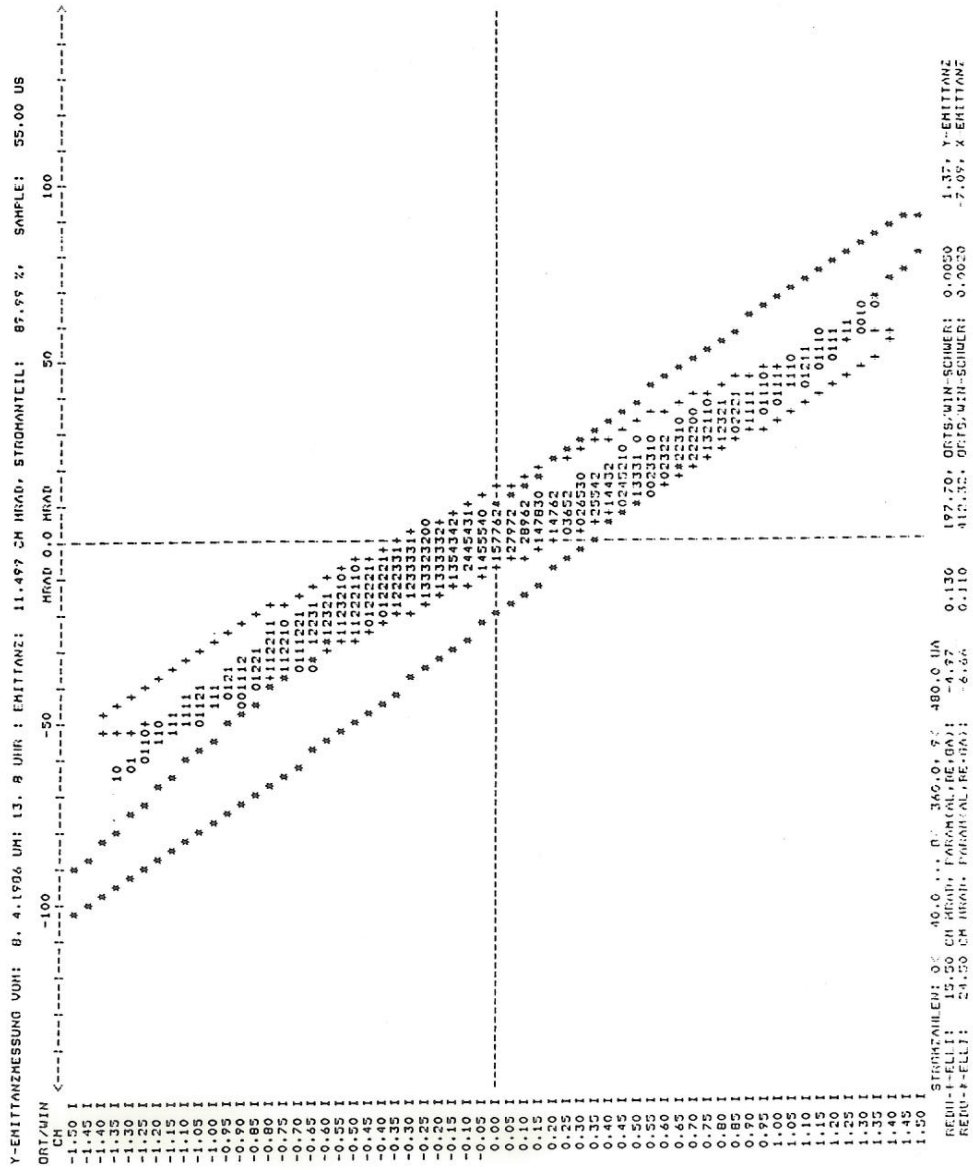
Y-EMITTANZMESSUNG VOM: 8. 4.1986 UM: 13. 8 UHR : EMITTANZ: 11.497 CM MRAD, STROMANTEIL: 87.99 %, SAMPLE: 55.00 US
ORT/WIN
CM
MRAD 0.0 MRAD
-100
-50
50
100
STROMKANALEN: 0
REDU-X-FELD: 15.50 CM MRAD, FARADAY-BEREICH: -4.87
REDU-Y-FELD: 24.50 CM MRAD, FARADAY-BEREICH: -6.66
0.130
0.110
197.70, ORTS-WIN-SCHWER: 0.0050
1.37, Y-EMITTANZ
-7.09, X-EMITTANZ

Fig. 4

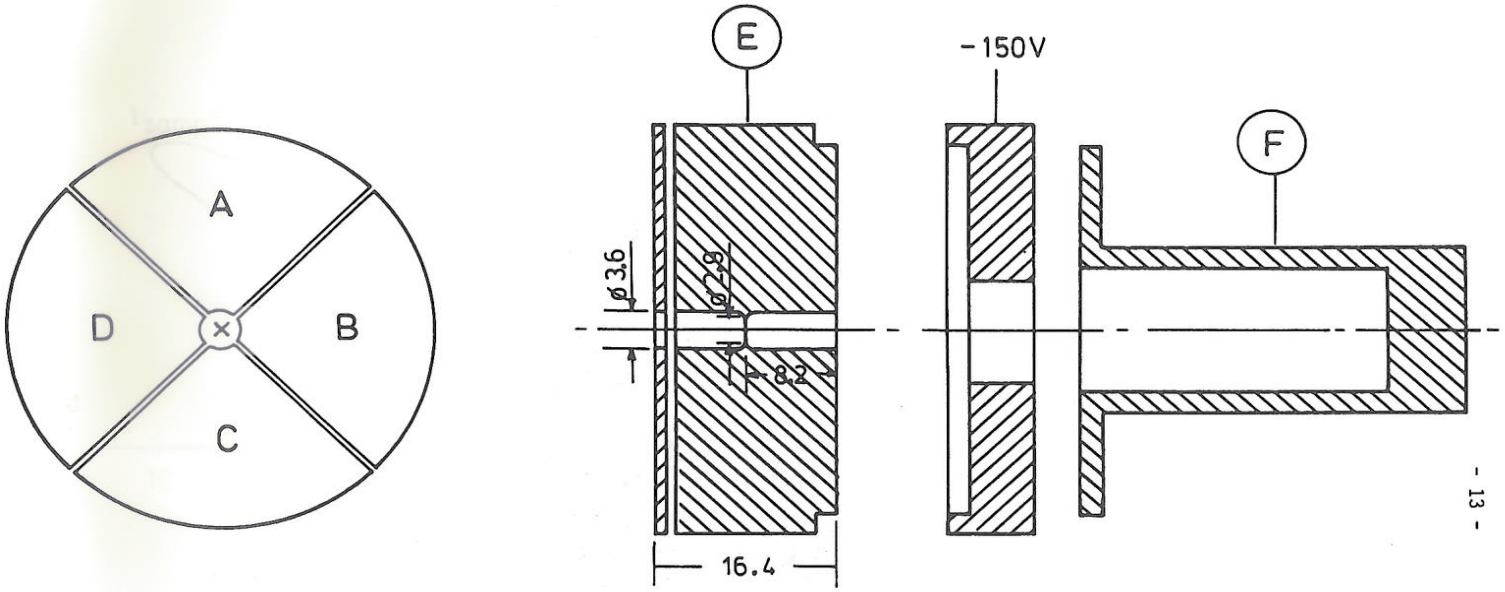
A
B
C
D
E
F
-150V
ø3.6
ø22.6
8.2
16.4

Fig. 5

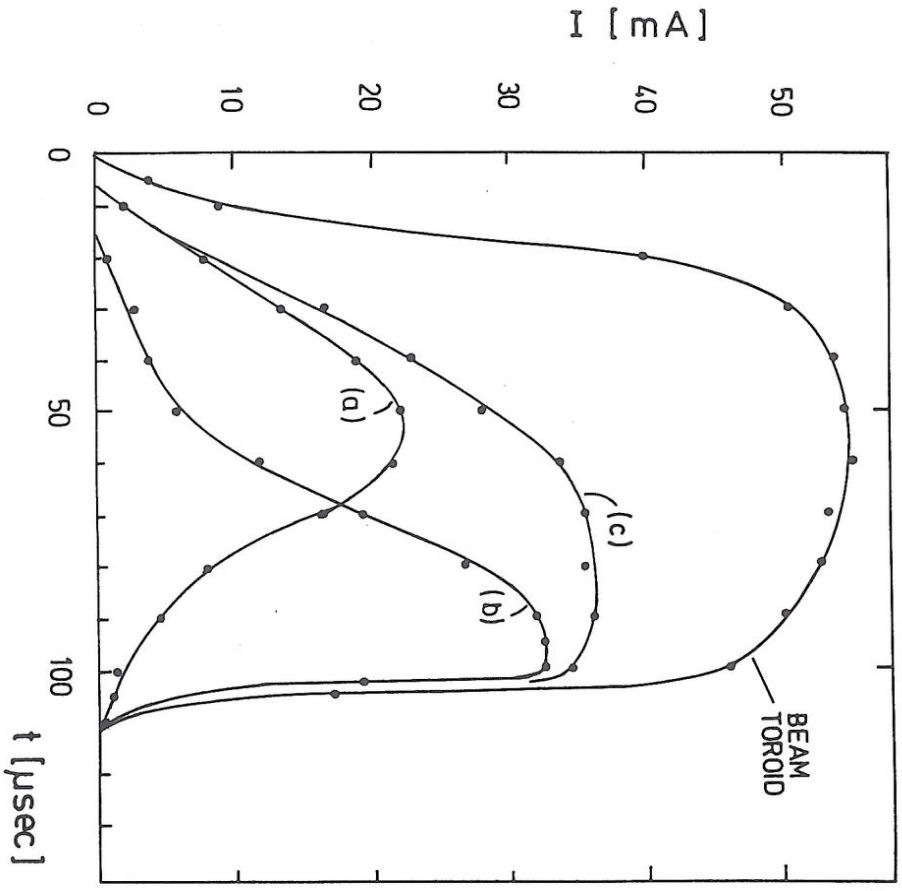
I [mA]
0
10
20
30
40
50
0
50
100
t [µsec]
(a)
(b)
(c)
BEAM
TOROID

Fig. 6

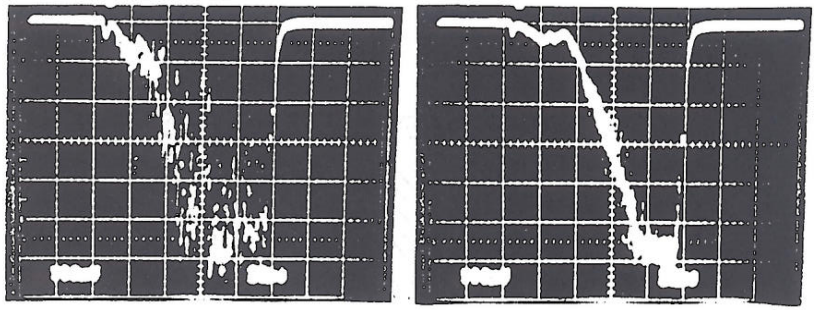

(a) (b)

Fig. 7

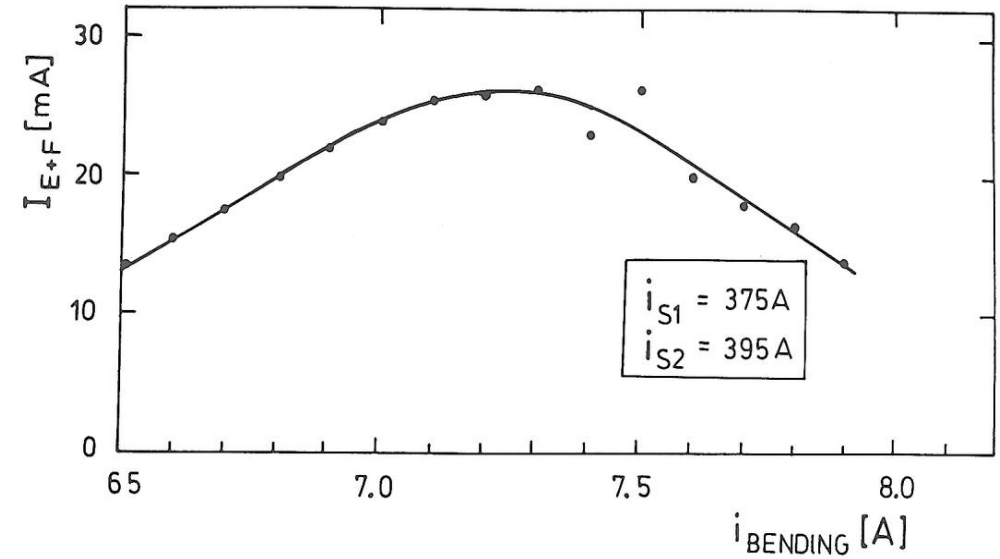
30
20
10
0
I_{E+F} [mA]
i_{S1} = 375A
i_{S2} = 395A
6 5
7.0
7. 5
8.0
$i_{BENDING}$ [A]

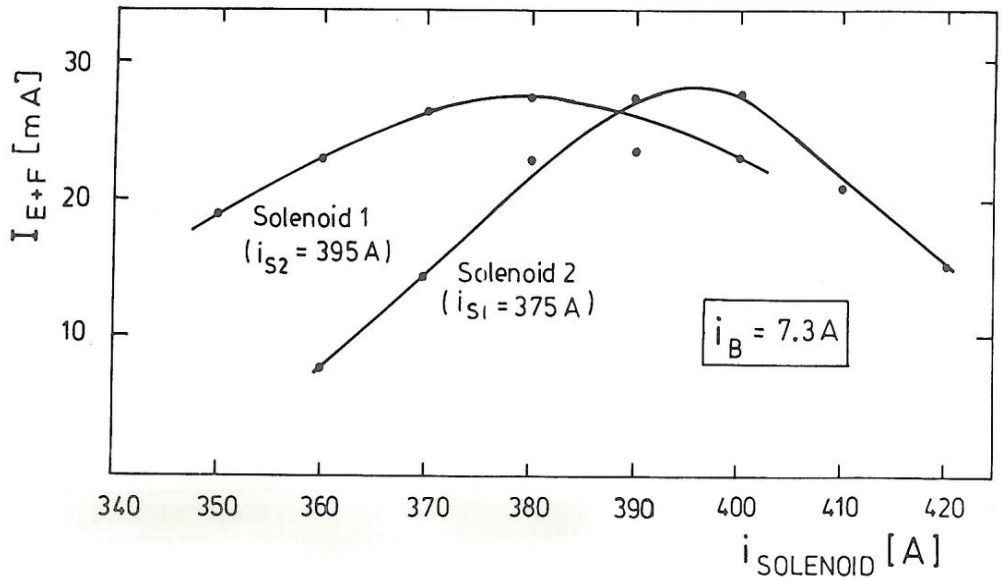
30
20
10
I_{E+F} [mA]
Solenoid 1
(i_{S2} = 395 A)
Solenoid 2
(i_{S1} = 375 A)
i_B = 7.3 A
340
350
360
370
380
390
400
410
420
$i_{SOLENOID}$ [A]

Fig. 8

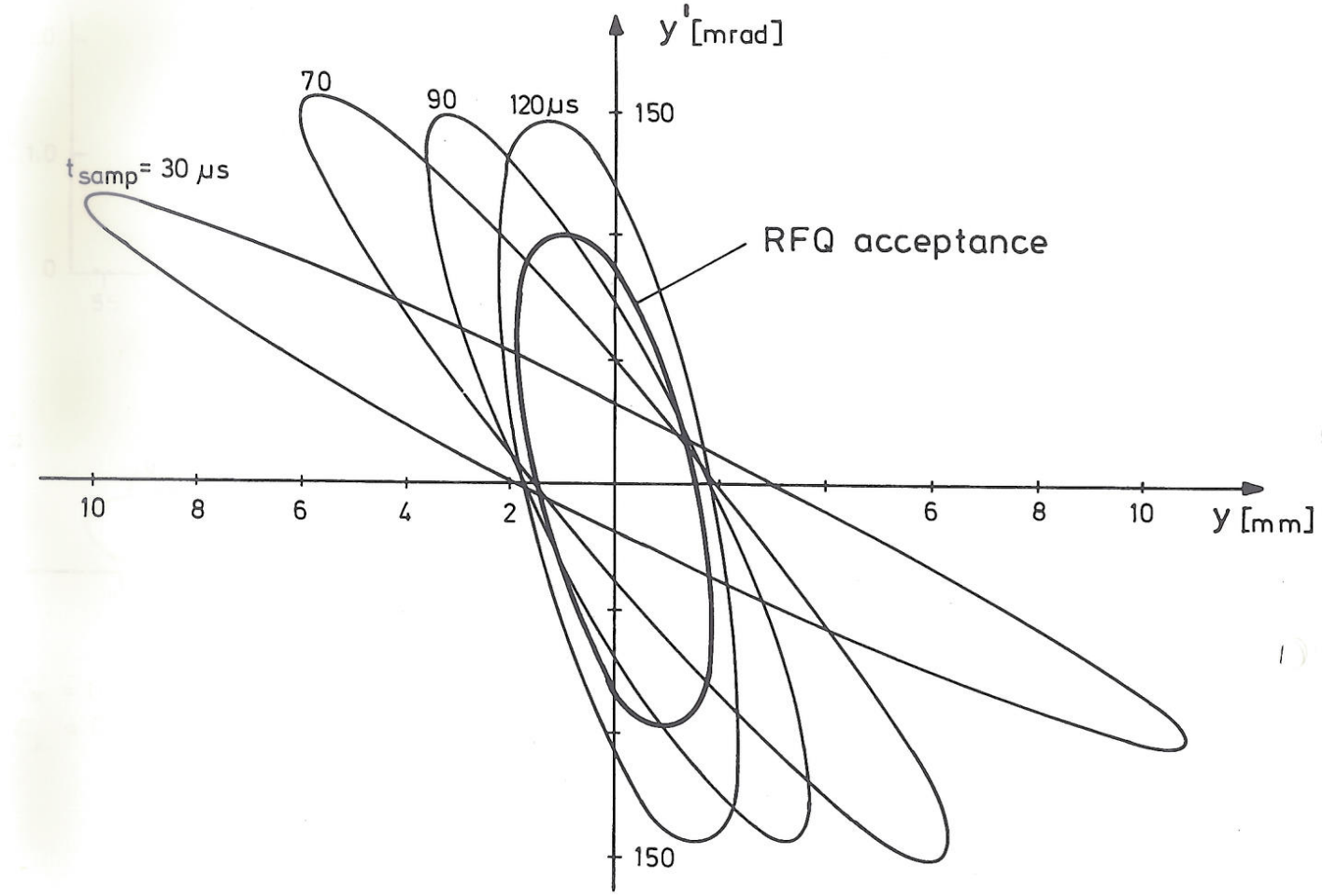
y' [mrad]
70
90
120 µs
150
t_{samp} = 30 µs
RFQ acceptance
10
8
6
4
2
6
8
10
y [mm]
150

Fig. 9

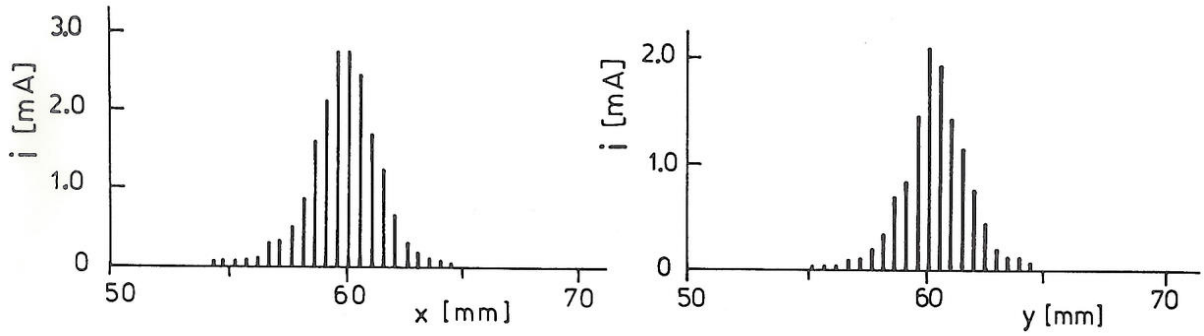
i [mA]
3.0
2.0
1.0
0
50
60
70
x [mm]
i [mA]
2.0
1.0
0
50
60
70
y [mm]

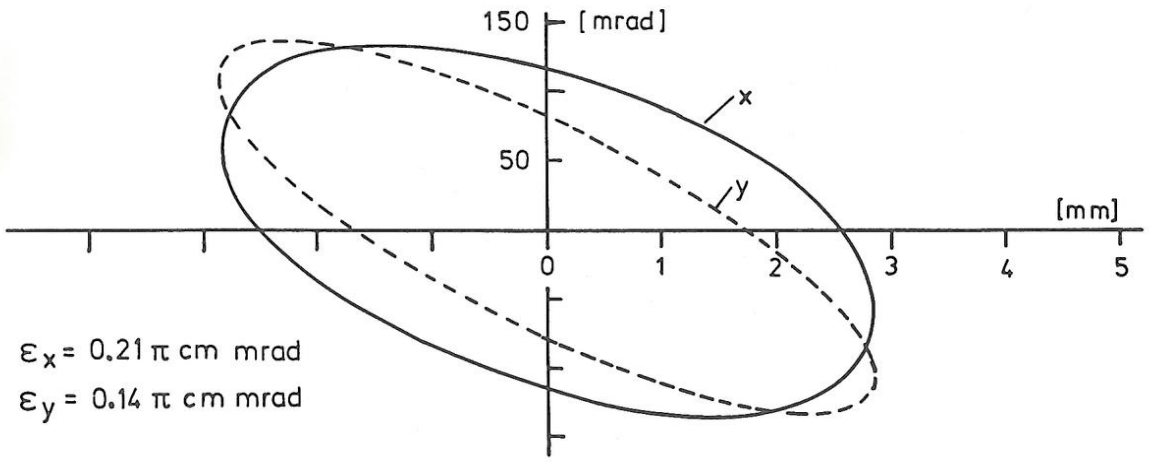
150
[mrad]
50
x
y
[mm]
0
1
2
3
4
5
ε_x = 0.21 π cm mrad
ε_y = 0.14 π cm mrad

Fig. 10

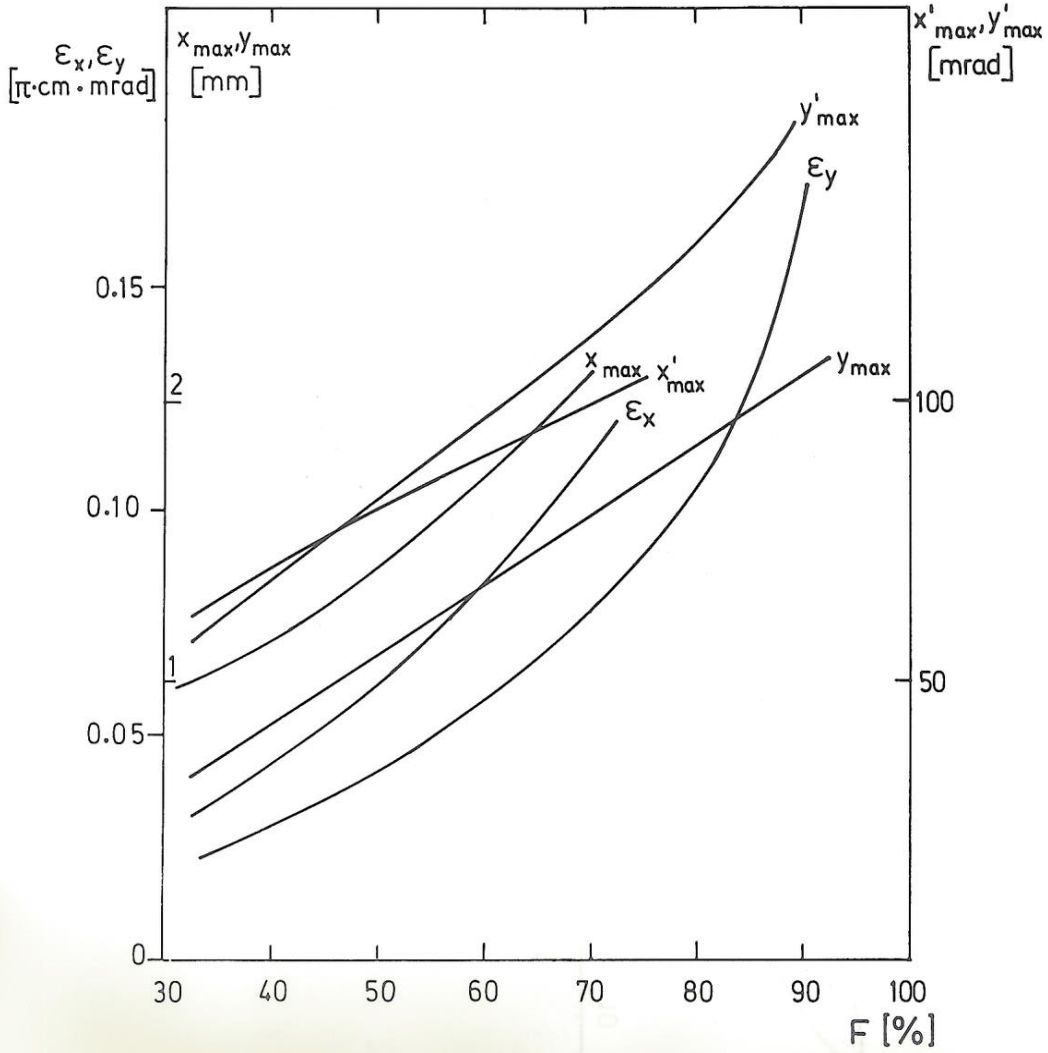
$\varepsilon_x, \varepsilon_y$ [π·cm·mrad]
x_{max}, y_{max} [mm]
x'_{max}, y'_{max} [mrad]
y'_{max}
ε_y
x_{max} x'_{max}
ε_x
y_{max}
0.15
0.10
0.05
0
2
1
100
50
30 40 50 60 70 80 90 100
F [%]

Fig. 11

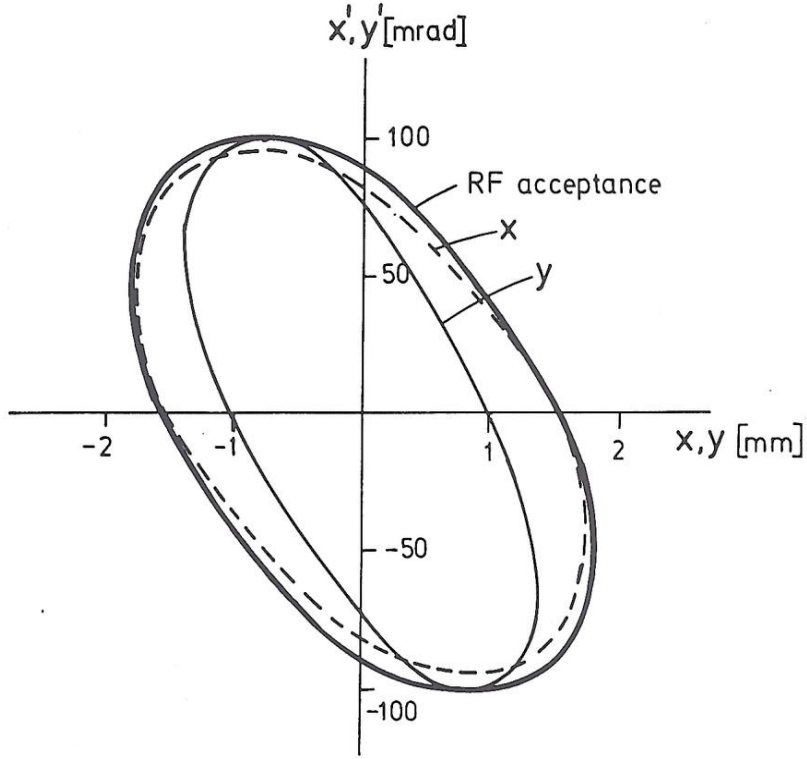
x', y' [mrad]
100
RF acceptance
x
50
y
-2
-1
1
2
x, y [mm]
-50
-100

Fig. 12

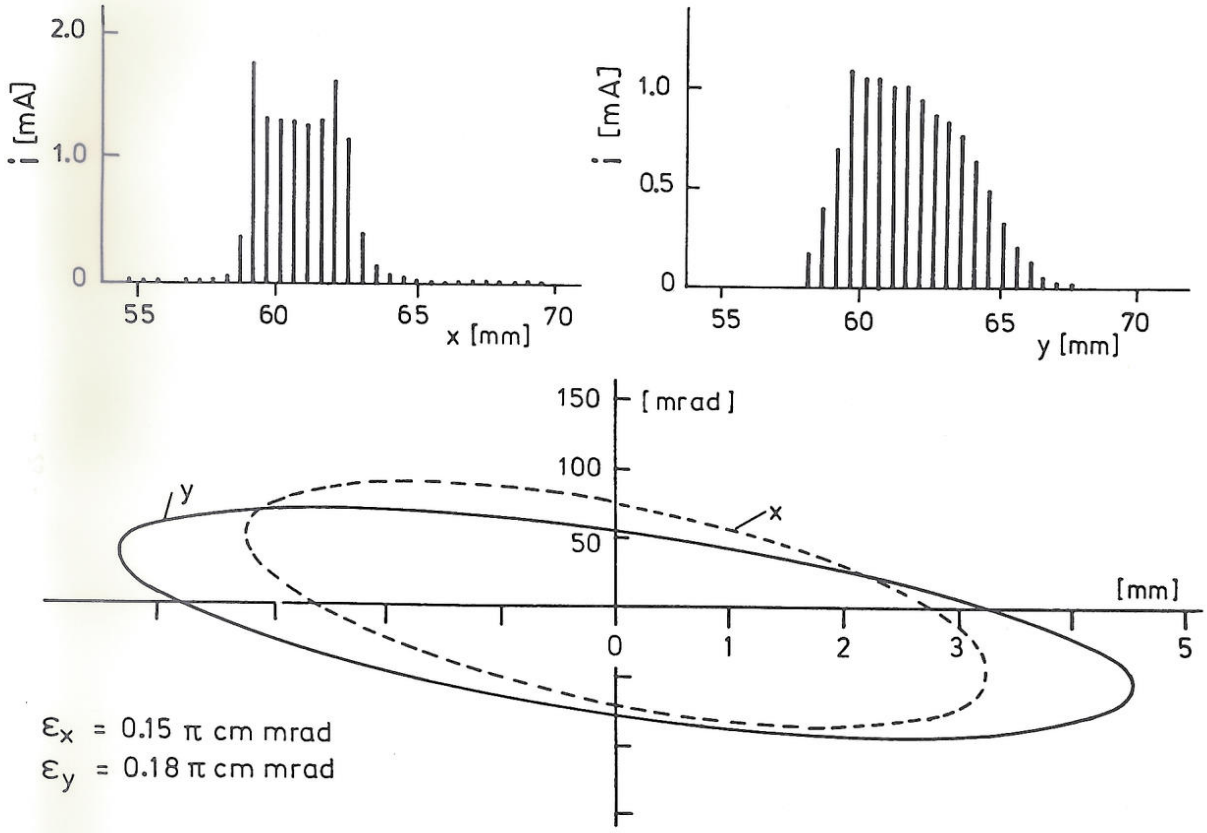
i [mA]
2.0
1.0
0
55
60
65
70
x [mm]
i [mA]
1.0
0.5
0
55
60
65
70
y [mm]
150
[mrad]
100
50
y
x
[mm]
0
1
2
3
5
ε_x = 0.15 π cm mrad
ε_y = 0.18 π cm mrad

Fig. 13

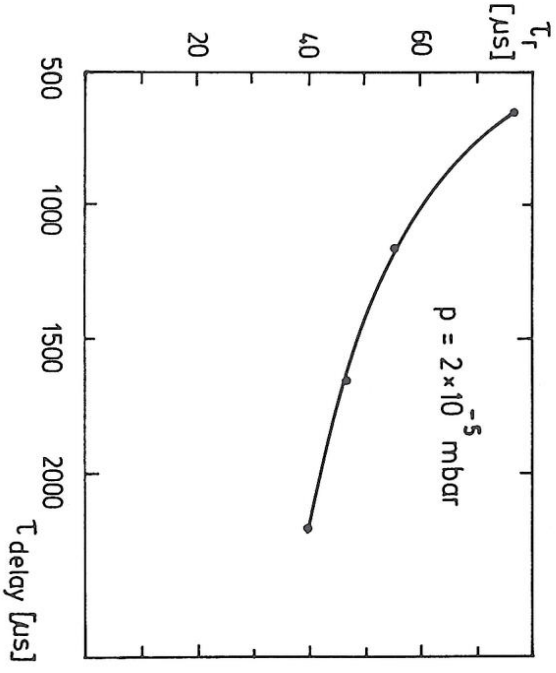
τ_r [µs]
20
40
60
500
1000
1500
2000
τ_{delay} [µs]
p = 2×10^{-5} mbar

Fig. 14

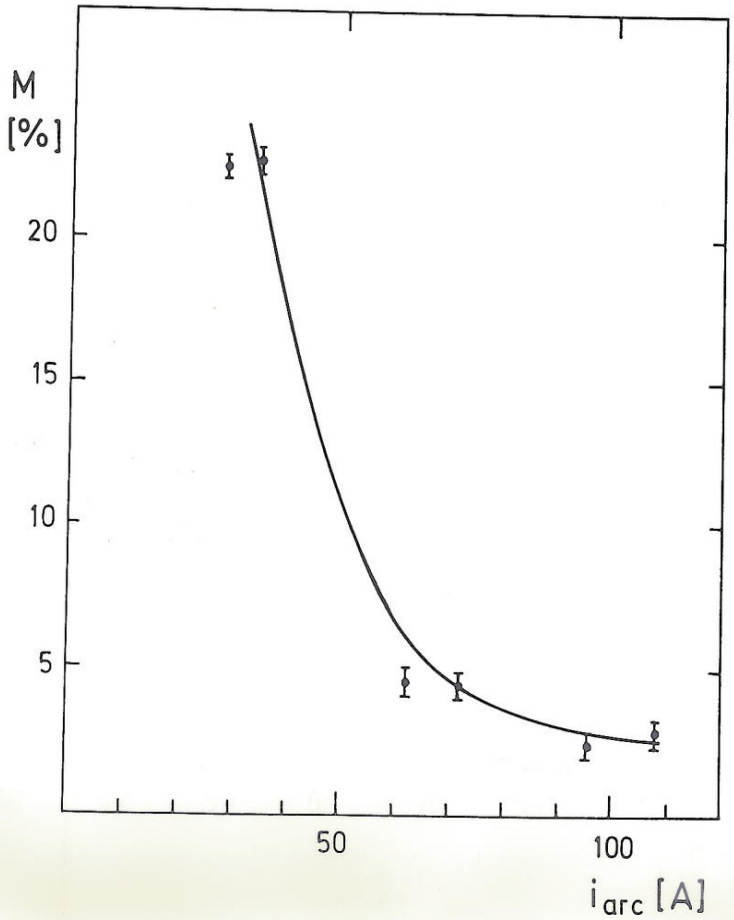

Fig.15